



HHS Public Access

Author manuscript

Bioconjug Chem. Author manuscript; available in PMC 2016 March 01.

Published in final edited form as:

Bioconjug Chem. 2015 August 19; 26(8): 1513–1518. doi:10.1021/acs.bioconjchem.5b00152.

Optimized Near-IR fluorescent agents for *in vivo* imaging of Btk expression

Eunha Kim[†], Katherine S. Yang[†], Rainer H. Kohler[†], John M. Dubach[†], Hannes Mikula[†], and Ralph Weissleder^{†,‡,*}

[†]Center for Systems Biology, Massachusetts General Hospital, 185 Cambridge St, CPZN 5206, Boston, MA 02114

[‡]Department of Systems Biology, Harvard Medical School, 200 Longwood Ave, Boston, MA 02115

Abstract

Bruton's tyrosine kinase (Btk) is intricately involved in anti-apoptotic signaling pathways in cancer and in regulating innate immune response. A number of Btk inhibitors are in development for use in treating B-cell malignancies and certain immunologic diseases. To develop robust companion imaging diagnostics for *in vivo* use, we set up to explore the effects of red wavelength fluorochrome modifications of two highly potent irreversible Btk inhibitors, Ibrutinib and AVL-292. Surprisingly, we found that subtle chemical differences in the fluorochrome had considerable effects on target localization. Based on iterative designs, we developed a single optimized version with superb *in vivo* imaging characteristics enabling single cell Btk imaging *in vivo*. This agent (Ibrutinib-SiR-COOH) is expected to be valuable chemical tool in deciphering Btk biology in cancer and host cells *in vivo*.

Keywords

Btk; Ibrutinib; Silicon-rhodamine; fluorochromes; microscopy; imaging

Introduction

The Btk (Bruton's tyrosine kinase) protein is a non-receptor tyrosine kinase essential in B-cell development,^{1, 2} B- and mast cell activation³ and macrophage signaling.^{4, 5} Btk is the upstream activator of multiple antiapoptotic signaling molecules and networks and prevents the interaction of Fas with Fas-associated protein with death domain (FADD).⁶ Btk is highly expressed in multiple myeloma,⁷ acute myeloid leukemia (AML),⁸ chronic lymphocytic leukemia (CLL),⁹ and non-Hodgkin's lymphoma (NHL).^{10, 11} Given its importance, Btk has emerged as a molecular target for treatment of B-lineage leukemias and lymphomas. In

*R. Weissleder, MD, PhD, Center for Systems Biology, Massachusetts General Hospital, 185 Cambridge St, CPZN 5206, Boston, MA 02114, 617-726-8226, rweissleder@mgh.harvard.edu.

Associated Content

Supporting Information Available: Procedures for chemical synthesis, compound characterization data, fluorescence spectra, procedures for cell line construction, SDS-PAGE, and *in vitro/in vivo* imaging, additional Figures. This information is available free of charge via <http://pubs.acs.org>.

addition, Btk plays a key role in macrophage polarization through signaling downstream of TLR4.¹² Btk also signals through TLR to control macrophage-mediated phagocytosis for programmed cell removal and pathogen clearing.^{13, 14} Given the importance of macrophage subsets in tumor development and progression,^{15, 16} as well as in other chronic diseases,¹⁷ it appears that Btk inhibition may offer a new therapeutic approach in modulating macrophage populations.^{18, 19}

One Btk inhibitor is clinically approved (Ibrutinib) while others are under development.^{20–23} Ibrutinib (PCI-32765) is a selective, irreversible Btk inhibitor, due to electrophilic group binding to Cys 481 in the active site of Btk.²⁴ This covalent binding results in long-lasting (> 24 hrs) target occupancy.^{25, 26} AVL-292, is an alternative, highly selective covalent Btk inhibitor, based on a dianilinopyrimidine backbone.

The continued development and clinical applications of newer Btk inhibitors would benefit from companion Btk imaging agents. Such tools could be especially valuable to better understand the kinetics, selectivity, drug action, dose ranging or allow *in vitro* testing of drug occupancy on harvested cells from patients for personalized medicine. We have previously reported on a BODIPY modified Ibrutinib, originally designed for cell culture work.²⁷ While this companion imaging drug worked reasonably well *in vitro*, *in vivo* imaging was much more challenging. Ibrutinib-BFL imaging required high doses and resulted in much lower than expected target-to-background signal ratios as would have been expected from *in vitro* results. Since these results were unanticipated and prevented high-resolution single cell analytical studies, especially *in vivo*, we set out to develop alternative *in vivo* imaging agents with better pharmacokinetics and imaging characteristics. We were particularly interested in red-shifted fluorochromes that would be complementary to typically used GFP labels in mouse models. We first tested a number of commercially available fluorochromes attached to the Ibrutinib and AVL-292 scaffold. Most of these conjugates also resulted in low binding affinity and suboptimal imaging characteristics. In search for red-shifted alternative fluorochromes, we finally tested silicon based fluorochromes such as SiR-Me,²⁸ with similar results. Quite unexpectedly, we found that a simple carboxylation of Si structures resulted in conjugates with superb *in vivo* imaging characteristics.

Results

To develop fluorescent Btk companion imaging drugs (CID) for *in vivo* use, we chose two highly potent and selective covalent inhibitors, Ibrutinib and AVL-292 with sub-nanomolar inhibitory activities.²⁹ Based on some previous studies with PCI-33380²⁵ as well as other Ibrutinib conjugates^{27, 30, 31} allowed us to identify two different positions for fluorochrome modification with minimal perturbation of the original binding sites. Based on these designs, we first synthesized the amine versions of Ibrutinib²⁷ (compound 6 ; Scheme 1), and AVL-292 (compound 21 ; Scheme S1), using slightly modified reported procedures.²² These amine compounds were then used for subsequent modification with different fluorochromes (Tables 1, Figure 1). Specifically, we chose 6 different fluorochromes (SiR-COOH, SiR-Me, FITC, Rhodamine Green, BODIPY-650, and BFL) with different chemical properties, as well as different emission wavelengths (Table 1). All CIDs were first screened

using HT1080 cell lines stably expressing Btk-mCherry, to examine the co-localization between drug and Btk protein. Interestingly, only 3 of the 8 compounds (Ibrutinib-SiR-COOH, Ibrutinib-BFL and AVL-292-SiR-COOH) showed reproducible co-localization with a Pearson coefficient above 0.9 (Table 1, Figure 2, Figure S1, Figure S2, Figure S3). High resolution live cell imaging provided insight into the cellular localization of the CIDs. Ibrutinib conjugates of fluorescein and rhodamine green were not cell permeable (Figure S7, Figure S8).

We postulate that this is likely because of the net negative charge of the conjugates. Conversely, the more hydrophobic imaging agents (Ibrutinib-BODIPY 650 and AVL-292-BFL, cLogP >7) showed significant background signal (Figure S5, Figure S6) presumably due to nonspecific binding in undesired subcellular compartments. Interestingly, Ibrutinib-SiR-Me localized to the mitochondria rather than the cytoplasm where Btk is located (Figure S4). We suspected that this unique distribution was due to charge effects of the fluorochrome (net charge = +1).³² To counteract the positive charge we next tested Ibrutinib-SiR-COOH, (Figure 1, Figure S1). Ibrutinib-SiR-COOH (Figure 2) and AVL-292-SiR-COOH (Figure S9a) both have a net neutral charge,³³⁻³⁵ a cLogP <5, submicromolar IC₅₀ (Ibrutinib-SiR-COOH = 122.8 nM and AVL-292-SiR-COOH = 283.5 nM, Figure S10) and showed excellent co-localization with Btk *in vitro*.

Given the unique properties of Ibrutinib-SiR-COOH, we next performed an in depth analysis of the CID. We first confirmed covalent protein binding of Ibrutinib-SiR-COOH by SDS-PAGE using purified Btk protein (Figure 3a, Figure S11a). We confirmed that the CID labeled purified Btk protein in a dose dependent manner. Selectivity of the imaging probe was next confirmed by SDS-PAGE gel experiments with Toledo (Btk positive B-cells) and Jurkat (Btk-negative T-cells) cell lines. As expected, Figure 3b shows a single fluorescent band in the whole cell lysate from the Toledo cells, but not from the Jurkat cells (Figure 3b, Figure S11b). This selectivity was also confirmed with FACS analysis as well as live cell fluorescent imaging experiments (Figure S12). Furthermore, drug occupancy of unlabeled Ibrutinib in Btk was monitored with Ibrutinib-SiR-COOH. Toledo cells were first treated with different doses of unlabeled Ibrutinib for 30 min, followed by 500 nM Ibrutinib-SiR-COOH for 3h. SDS-PAGE of the Toledo whole cell lysate clearly showed unlabeled Ibrutinib occupancy of Btk in a dose dependent manner using fluorescent gel scanning. Overall we confirmed covalent binding and exquisite selectivity of Ibrutinib-SiR-COOH against Btk. This unique property allows for potential application of the CID in drug response monitoring.

In the next set of experiments, we tested the lead compound (Ibrutinib-SiR-COOH) and two close competitors (Ibrutinib-BFL and AVL292-SiR-COOH) in mice to determine the pharmacokinetics and imaging characteristics. Ibrutinib-SiR-COOH had a vascular t_{1/2} of 18 minutes (Figure 4). Ninety minutes after intravenous injection, all vascular fluorescent signal had decreased to background. To determine co-localization *in vivo*, we used window chambers in mice under which we grew mixed populations of HT1080-Btk-mCherry (Btk+) and HT1080-H2B-GFP cells (Btk-) as tumor masses. Ibrutinib-SiR-COOH showed excellent co-localization with Btk-mCherry in HT1080 cells (Figure 5). There was no

background fluorescent signal in HT1080 cells lacking Btk, even 24 h after IV administration (Figure S13).

Identical experiments with the other two compounds (Ibrutinib-BFL²⁷ and AVL292-SiR-COOH; Figure S14) resulted in far inferior images with significant background.

Discussion

We synthesized 6 different fluorochrome based Btk imaging agents and showed that several of these compounds exhibit reasonable imaging characteristics and co-localization with Btk-mCherry in cell culture. However, only one compound (Ibrutinib-SiR-COOH) showed pharmacokinetics and target location, enabling Btk specific single cell imaging. The lead compound is based on a carboxylated silicone fluorochrome covalently linked to the irreversible Btk inhibitor Ibrutinib. Interestingly, elimination of a single carboxylate group on the fluorochrome essentially abrogated Btk binding. Compared to the previously described green Ibrutinib-BFL,²⁷ the red-shifted lead compound exhibits superior binding and imaging characteristics, due to improved pharmacokinetics, lower background accumulation and red-shifted imaging with lower autofluorescence *in vivo*.

The developed CID potentially has a broad range of applications, including spatial profiling of Btk expression in malignancies or other inflammatory tissues, measurement of receptor inhibition with competing non-fluorescent compounds, pharmacokinetic and pharmacodynamic studies at the single cell level or *in vivo* studies to elucidate Btk biology. Irrespective of the specific application, we believe that the developed compound will be of considerable interest.

Supplementary Material

Refer to Web version on PubMed Central for supplementary material.

Acknowledgments

We are grateful to David Pirovich for imaging assistance and Dr. Ralph Mazitschek for many helpful discussions. The authors acknowledge funding from National Institutes of Health (NIH) grants T32CA079443 and P50CA086355, and in part by R01EB010011.

In compliance with Partners Healthcare/Harvard Medical School institutional guidelines, R.W. discloses his financial interest in Lumicell, a biotechnology company developing intraoperative imaging systems for surgical applications. Lumicell did not support the research herein, and the company has no rights to any technology or intellectual property developed as part of this research.

References

1. de Weers M, Brouns GS, Hinshelwood S, Kinnon C, Schuurman RK, Hendriks RW, Borst J. B-cell antigen receptor stimulation activates the human Bruton's tyrosine kinase, which is deficient in X-linked agammaglobulinemia. *J Biol Chem.* 1994; 269:23857–23860. [PubMed: 7929028]
2. Rawlings DJ, Saffran DC, Tsukada S, Largaespada DA, Grimaldi JC, Cohen L, Mohr RN, Bazan JF, Howard M, Copeland NG, et al. Mutation of unique region of Bruton's tyrosine kinase in immunodeficient XID mice. *Science.* 1993; 261:358–361. [PubMed: 8332901]

3. Kawakami Y, Kitaura J, Hartman SE, Lowell CA, Siraganian RP, Kawakami T. Regulation of protein kinase C β I by two protein-tyrosine kinases, Btk and Syk. *Proc Natl Acad Sci USA*. 2000; 97:7423–7428. [PubMed: 10852954]
4. Gray P, Dunne A, Brikos C, Jefferies CA, Doyle SL, O'Neill LA. MyD88 Adapter-like (Mal) is phosphorylated by Bruton's tyrosine kinase during TLR2 and TLR4 signal transduction. *J Biol Chem*. 2006; 281:10489–10495. [PubMed: 16439361]
5. Liljeroos M, Vuolteenaho R, Morath S, Hartung T, Hallman M, Ojaniemi M. Bruton's tyrosine kinase together with PI 3-kinase are part of Toll-like receptor 2 multiprotein complex and mediate LTA induced Toll-like receptor 2 responses in macrophages. *Cell Signal*. 2007; 19:625–633. [PubMed: 17020802]
6. Vassilev A, Ozer Z, Navara C, Mahajan S, Uckun FM. Bruton's tyrosine kinase as an inhibitor of the Fas/CD95 death-inducing signaling complex. *J Biol Chem*. 1999; 274:1646–1656. [PubMed: 9880544]
7. Tai YT, Anderson KC. Bruton's tyrosine kinase: oncotarget in myeloma. *Oncotarget*. 2012; 3:913–914. [PubMed: 22989914]
8. Rushworth SA, Murray MY, Zaitseva L, Bowles KM, MacEwan DJ. Identification of Bruton's tyrosine kinase as a therapeutic target in acute myeloid leukemia. *Blood*. 2014; 123:1229–1238. [PubMed: 24307721]
9. Woyach JA, Bojnik E, Ruppert AS, Stefanovski MR, Goettl VM, Smucker KA, Smith LL, Dubovsky JA, Towns WH, MacMurray J, et al. Bruton's tyrosine kinase (BTK) function is important to the development and expansion of chronic lymphocytic leukemia (CLL). *Blood*. 2014; 123:1207–1213. [PubMed: 24311722]
10. Bogusz AM, Baxter RH, Currie T, Sinha P, Sohani AR, Kutok JL, Rodig SJ. Quantitative immunofluorescence reveals the signature of active B-cell receptor signaling in diffuse large B-cell lymphoma. *Clin Cancer Res*. 2012; 18:6122–6135. [PubMed: 22966017]
11. Cinar M, Hamedani F, Mo Z, Cinar B, Amin HM, Alkan S. Bruton tyrosine kinase is commonly overexpressed in mantle cell lymphoma and its attenuation by Ibrutinib induces apoptosis. *Leuk Res*. 2013; 37:1271–1277. [PubMed: 23962569]
12. Ni Gabhann J, Hams E, Smith S, Wynne C, Byrne JC, Brennan K, Spence S, Kissenpfennig A, Johnston JA, Fallon PG, et al. Btk regulates macrophage polarization in response to lipopolysaccharide. *PLoS One*. 2014; 9:e85834. [PubMed: 24465735]
13. Feng M, Chen JY, Weissman-Tsakamoto R, Volkmer JP, Ho PY, McKenna KM, Cheshier S, Zhang M, Guo N, Gip P, et al. Macrophages eat cancer cells using their own calreticulin as a guide: Roles of TLR and Btk. *Proc Natl Acad Sci USA*. 2015; 112:2145–2150. [PubMed: 25646432]
14. Herbst S, Shah A, Mazon Moya M, Marzola V, Jensen B, Reed A, Birrell MA, Saijo S, Mostowy S, Shaunak S, et al. Phagocytosis-dependent activation of a TLR9–BTK–calcineurin–NFAT pathway co-ordinates innate immunity to *Aspergillus fumigatus*. *EMBO Mol Med*. 2015; 7:240–258. [PubMed: 25637383]
15. Ruffell B, Affara NI, Coussens LM. Differential macrophage programming in the tumor microenvironment. *Trends Immunol*. 2012; 33:119–126. [PubMed: 22277903]
16. Hao NB, Lu MH, Fan YH, Cao YL, Zhang ZR, Yang SM. Macrophages in tumor microenvironments and the progression of tumors. *Clin Dev Immunol*. 2012; 2012:948098. [PubMed: 22778768]
17. Kinne RW, Brauer R, Stuhlmuller B, Palombo-Kinne E, Burmester GR. Macrophages in rheumatoid arthritis. *Arthritis Res*. 2000; 2:189–202. [PubMed: 11094428]
18. Hartkamp LM, Fine JS, van Es IE, Tang MW, Smith M, Woods J, Narula S, Demartino J, Tak PP, Reedquist KA. Btk inhibition suppresses agonist-induced human macrophage activation and inflammatory gene expression in RA synovial tissue explants. *Ann Rheum Dis*. 2014; 10.1136/annrheumdis-2013-204143
19. Zhou P, Ma B, Xu S, Zhang S, Tang H, Zhu S, Xiao S, Ben D, Xia Z. Knockdown of Bruton's tyrosine kinase confers potent protection against sepsis-induced acute lung injury. *Cell Biochem Biophys*. 2014; 70:1265–1275. [PubMed: 24906236]

20. Advani RH, Buggy JJ, Sharman JP, Smith SM, Boyd TE, Grant B, Kolibaba KS, Furman RR, Rodriguez S, Chang BY, et al. Bruton tyrosine kinase inhibitor Ibrutinib (PCI-32765) has significant activity in patients with relapsed/refractory B-cell malignancies. *J Clin Oncol*. 2013; 31:88–94. [PubMed: 23045577]
21. Byrd JC, Furman RR, Coutre SE, Flinn IW, Burger JA, Blum KA, Grant B, Sharman JP, Coleman M, Wierda WG, et al. Targeting BTK with Ibrutinib in relapsed chronic lymphocytic leukemia. *N Engl J Med*. 2013; 369:32–42. [PubMed: 23782158]
22. Evans EK, Tester R, Aslanian S, Karp R, Sheets M, Labenski MT, Witowski SR, Lounsbury H, Chaturvedi P, Mazdiyasi H, et al. Inhibition of Btk with CC-292 provides early pharmacodynamic assessment of activity in mice and humans. *J Pharmacol Exp Ther*. 2013; 346:219–228. [PubMed: 23709115]
23. Wang ML, Rule S, Martin P, Goy A, Auer R, Kahl BS, Jurczak W, Advani RH, Romaguera JE, Williams ME, et al. Targeting BTK with Ibrutinib in relapsed or refractory mantle-cell lymphoma. *N Engl J Med*. 2013; 369:507–516. [PubMed: 23782157]
24. Lou Y, Owens TD, Kuglstatler A, Kondru RK, Goldstein DM. Bruton's tyrosine kinase inhibitors: Approaches to potent and selective inhibition, preclinical and clinical evaluation for inflammatory diseases and B cell malignancies. *J Med Chem*. 2012; 55:4539–4550. [PubMed: 22394077]
25. Honigberg LA, Smith AM, Sirisawad M, Verner E, Lounsbury H, Chang B, Li S, Pan Z, Thamm DH, Miller RA, et al. The Bruton tyrosine kinase inhibitor PCI-32765 blocks B-cell activation and is efficacious in models of autoimmune disease and B-cell malignancy. *Proc Natl Acad Sci USA*. 2010; 107:13075–13080. [PubMed: 20615965]
26. Liu Q, Sabnis Y, Zhao Z, Zhang T, Buhrlage SJ, Jones LH, Gray NS. Developing irreversible inhibitors of the protein kinase cysteinome. *Chem Biol*. 2013; 20:146–159. [PubMed: 23438744]
27. Turetsky A, Kim E, Kohler RH, Miller MA, Weissleder R. Single cell imaging of Bruton's tyrosine kinase using an irreversible inhibitor. *Sci Rep*. 2014; 4:4782. [PubMed: 24759210]
28. Koide Y, Urano Y, Hanaoka K, Piao W, Kusakabe M, Saito N, Terai T, Okabe T, Nagano T. Development of NIR fluorescent dyes based on Si-rhodamine for in vivo imaging. *J Am Chem Soc*. 2012; 134:5029–5031. [PubMed: 22390359]
29. Srinivasarao M, Galliford CV, Low PS. Principles in the design of ligand-targeted cancer therapeutics and imaging agents. *Nat Rev Drug Discov*. 2015; 14:203–219. [PubMed: 25698644]
30. Lanning BR, Whitby LR, Dix MM, Douhan J, Gilbert AM, Hett EC, Johnson TO, Joslyn C, Kath JC, Niessen S, et al. A road map to evaluate the proteome-wide selectivity of covalent kinase inhibitors. *Nat Chem Biol*. 2014; 10:760–767. [PubMed: 25038787]
31. Zhang Q, Liu H, Pan Z. A general approach for the development of fluorogenic probes suitable for no-wash imaging of kinases in live cells. *Chem Commun (Camb)*. 2014; 50:15319–15322. [PubMed: 25347137]
32. Kim E, Yang KS, Giedt RJ, Weissleder R. Red Si-rhodamine drug conjugates enable imaging in GFP cells. *Chem Commun (Camb)*. 2014; 50:4504–4507. [PubMed: 24663433]
33. Choi HS, Nasr K, Alyabyev S, Feith D, Lee JH, Kim SH, Ashitate Y, Hyun H, Patonay G, Streckowski L, et al. Synthesis and In Vivo Fate of Zwitterionic Near-Infrared Fluorophores. *Angew Chem Int Ed Engl*. 2011; 50:6258–6263. [PubMed: 21656624]
34. Grimm JB, English BP, Chen J, Slaughter JP, Zhang Z, Revyakin A, Patel R, Macklin JJ, Normanno D, Singer RH, et al. A general method to improve fluorophores for live-cell and single-molecule microscopy. *Nat Methods*. 2015; 12:244–250. [PubMed: 25599551]
35. Lukinavicius G, Umezawa K, Olivier N, Honigsmann A, Yang G, Plass T, Mueller V, Reymond L, Correa IRJ, Luo ZG, et al. A near-infrared fluorophore for live-cell super-resolution microscopy of cellular proteins. *Nat Chem*. 2013; 5:132–139. [PubMed: 23344448]

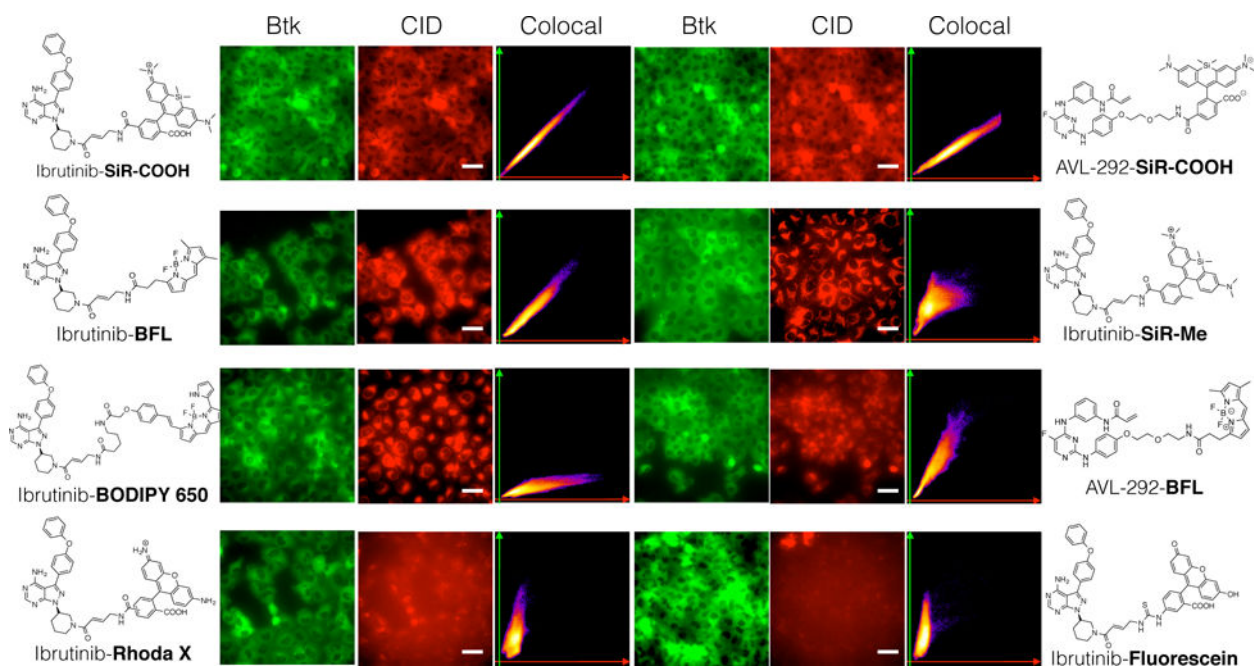


Figure 1. Comparison of 8 different CIDs

HT1080 cells expressing Btk-mCherry were incubated with 8 different imaging drugs (500 nM) for 2.5 hr. After washing the cells with growth medium 3 times for 5 minutes each, live cells were imaged using fluorescence microscopy. Scale bar: 50 μ m.

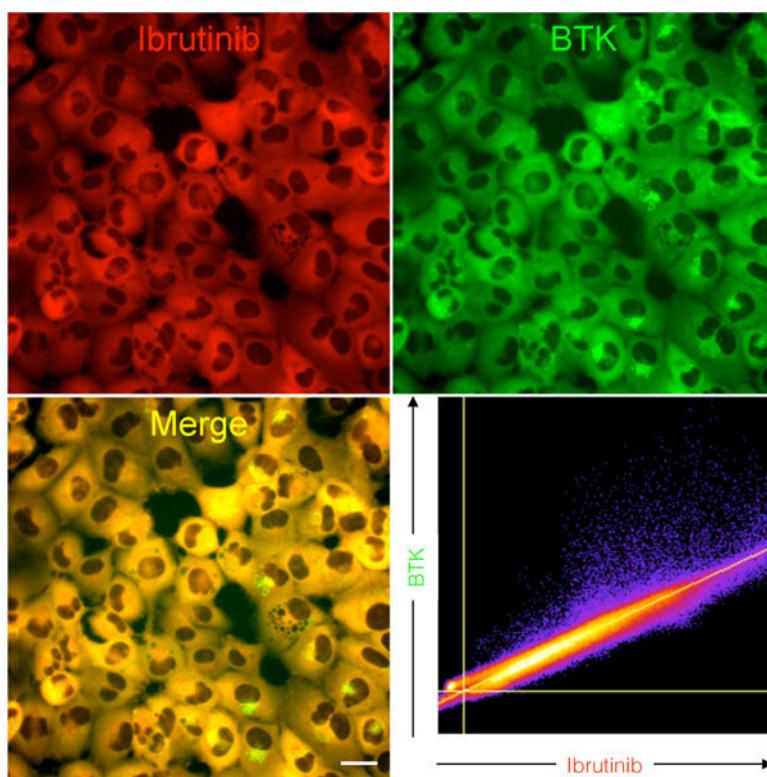


Figure 2. Higher resolution live cell microscopy of Btk-mCherry cells incubated with Ibrutinib-SiR-COOH

HT1080 cells stably transduced with Btk-mCherry (green) were imaged following a 3-hour incubation with Ibrutinib-SiR-COOH (500 nM). Note the exquisite co-localization between Ibrutinib-SiR-COOH and Btk-mCherry (Pearson's correlation coefficient is 0.98). Scale bar: 20 μm

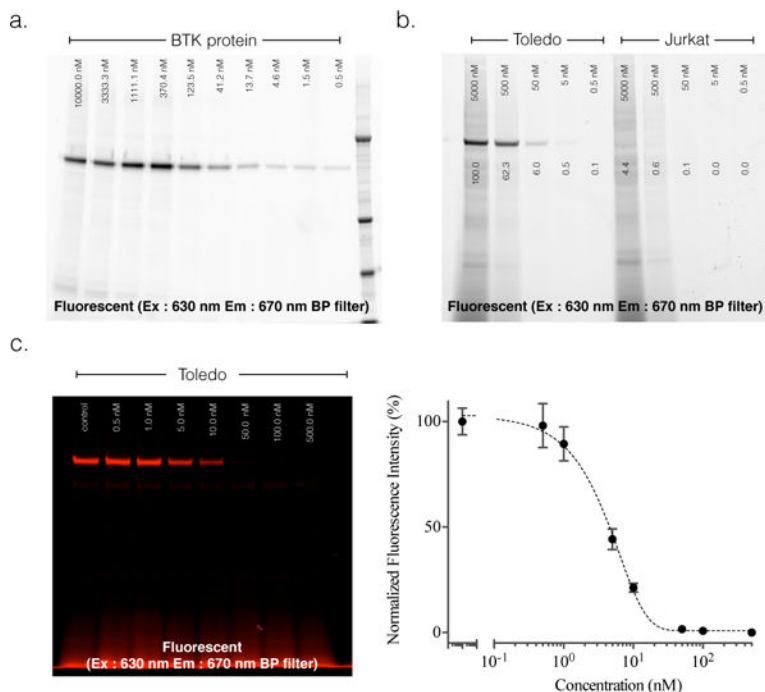


Figure 3. Covalent and Selective binding of Ibrutinib-SiR-COOH to Btk

a. Covalent target binding. Denaturing gel electrophoresis of decreasing concentrations of Ibrutinib-SiR-COOH incubated with 0.1 ng purified Btk for one hour and imaged with 630 nm excitation / 670 nm emission fluorescence gel scanning. Note the dose dependent binding of Ibrutinib-SiR-COOH. Molecular weight marker is in the far right lane. b. Selectivity of Ibrutinib-SiR-COOH against Btk in live cells. Denaturing gel electrophoresis of cell lysates following incubation of decreasing concentrations of Ibrutinib-SiR-COOH with Toledo (Btk+, left half of gel) or Jurkat (Btk-, right half of gel) cells at 37°C degrees for three hours. Note the superb specificity of the probe for Btk+ Toledo cells. c. Measurement of unlabeled Ibrutinib binding to Btk protein using the Ibrutinib-SiR-COOH CID. Denaturing gel electrophoresis of Toledo (Btk+) cell lysates following incubation of live cells with decreasing concentrations of Ibrutinib, followed by incubation with 500 nM of Ibrutinib-SiR-COOH.

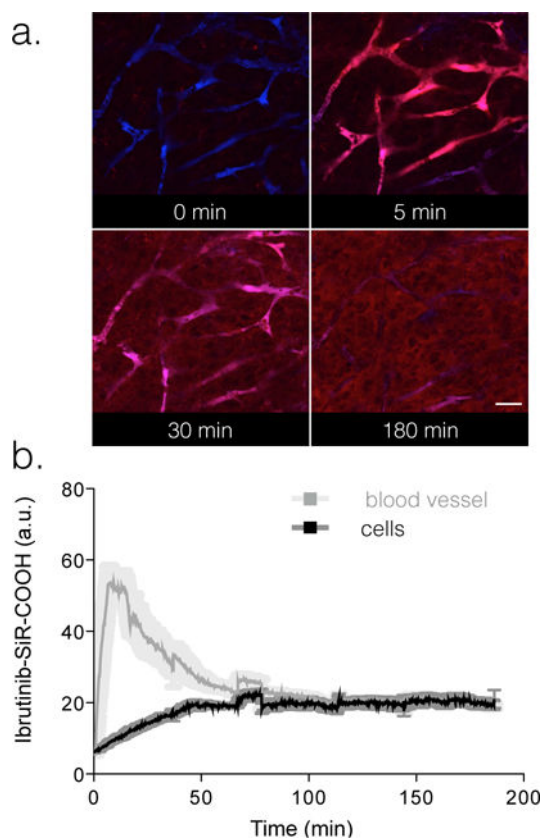


Figure 4. Vascular half-life of Ibrutinib-SiR-COOH

75 nmol Ibrutinib-SiR-COOH was injected into the tail vein of nu/nu mice and serial imaging was performed in the window chamber to determine vascular half-life of the injected probe. Imaging was performed using a customized Olympus FV1000 confocal/multiphoton microscope equipped with a 20 \times objective (both Olympus America, Chelmsford, MA, USA). a. Images of vasculature (FITC-Dextran) and Ibrutinib-SiR-COOH (red) over 180 minutes post injection. b. Fluorescence in the vasculature was used to calculate an initial blood half-life of Ibrutinib-SiR-COOH. Scale bar: 80 μ m.

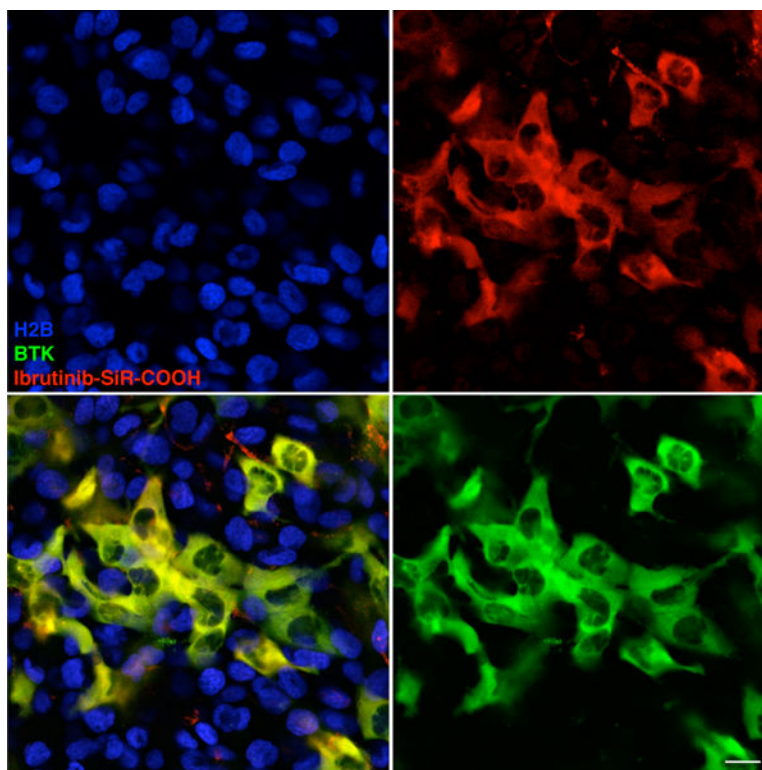


Figure 5. Single cell *in vivo* imaging of the Ibrutinib-SiR-COOH CID

Mice with a mixed HT1080 tumor containing both Btk negative and positive cells (green: Btk-mCherry cells, blue: H2B-GFP cells) were imaged 24 hours after i.v. administration of Ibrutinib-SiR-COOH (75 nmol). Note the excellent co-localization between the CID and Btk-mCherry, persisting even 24 hours post-injection. Scale bar: 20 μ m.

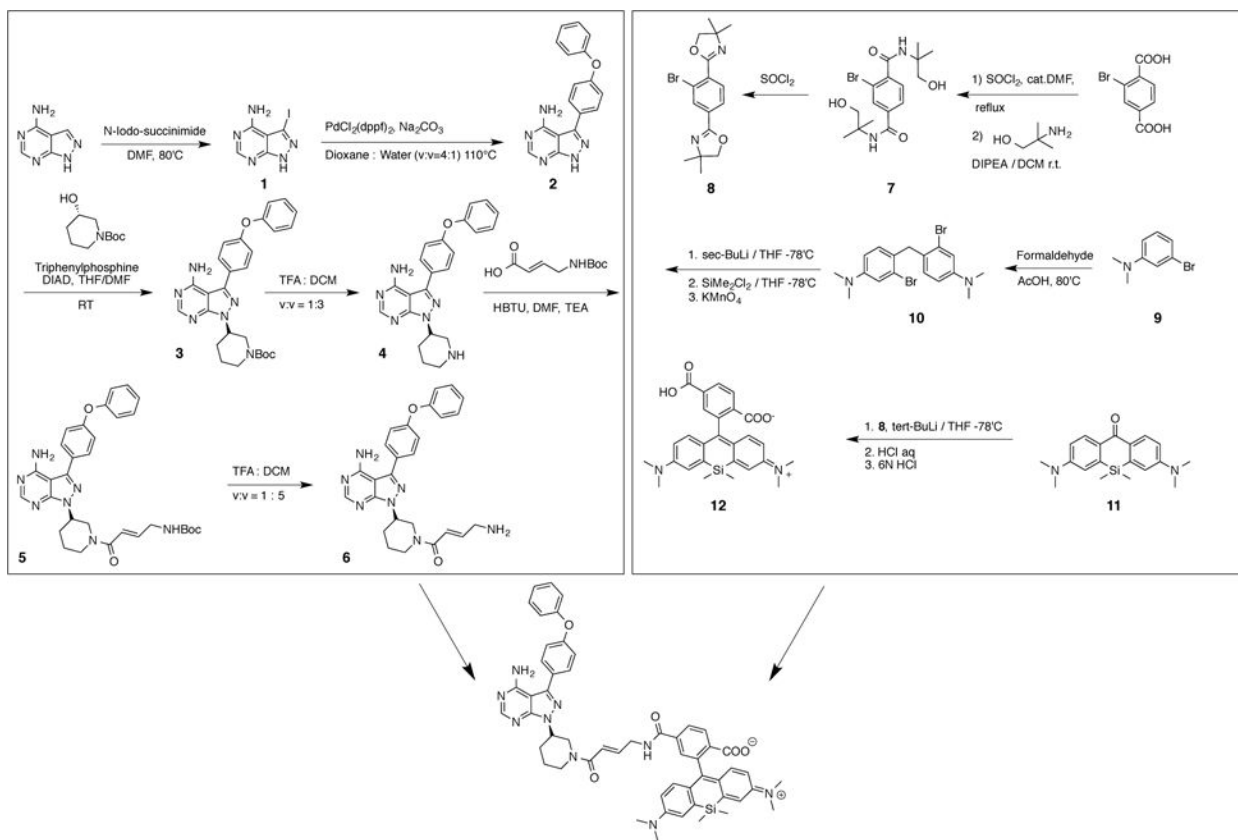


Table 1

Comparison of different CID

ND: not determined. +/++/+++ indicates the degree of colocalization.

	MW	cLogP	Ex/em	Co-loc in cells	T _{1/2} (min)	Co-loc in vivo
Ibrutinib-Si-COOH	924.40	2.4	651/671	+++	18.8	+++
Ibrutinib-Si-Me	894.43	7.1	653/670	-	ND	ND
Ibrutinib-B650	998.44	8.7	650/670	-	ND	ND
Ibrutinib-Rhx	826.31	0.3	500/534	-	ND	ND
Ibrutinib-BFL	743.33	6.7	504/516	++	11.3	+
Ibrutinib-FITC	859.27	-0.4	499/531	-	ND	ND
AVL-292-Si-COOH	907.39	2.8	646/668	+++	ND	-
AVL-292-BFL	727.31	7.8	504/514	++	ND	ND